CORONAL EMISSION AND STELLAR EVOLUTION

G. S. VAIANA
and
A. MAGGIO, G. MICELA, S. SCIORTINO
Osservatorio Astronomico di Palermo
Piazza del Parlamento 1, 90134 Palermo, Italy

Foreword
An oral version of this paper was given by G.S. Vaiana at the JCM on Solar and Stellar Coronae, held in Buenos Aires on July 31, 1991. Giuseppe S. Vaiana died untimely by a massive hearth attack on August 25 1991 leaving us without a great *maestro* and a dear friend. Following his notes and on the basis of the many discussions we had together, we have written this paper as an homage to his unforgettable memory.

A. Maggio, G. Micela, S. Sciortino

Abstract

This paper is an overview of the results of stellar X-ray astronomy at the closing of the *Einstein* and *EXOSAT* eras, and at the opening of the ROSAT era, with particular emphasis on the influence of stellar evolution on the X-ray emission from normal stars, and on the contribution of normal star X-ray emission to the X-ray makeup of the Galaxy.

1 Introduction

We will focus on those aspects of X-ray coronal emission of interest in stellar evolution. Ideally one would like to understand the origin of coronal emission in the perspective of stellar evolution, including the role of convection, magnetic field, and angular momentum. Everyone agrees that all this has something to do with coronal emission, but to understand in detail which mechanisms operate is a different matter.

The mechanism at the origin of coronal activity in late type stars is complex, and not yet fully clarified. It is thought to involve the stellar structure through the properties of the convective zone, rotation, and formation and dissipation of magnetic fields and turbulence: in general terms, a mechanism of the type qualitatively operating on the Sun (Parker 1979; Rosner, Low, and Holtzer 1986). In the following, we will summarize various evidences and quantitative determinations of evolutionary effects, based on data for classes of stars that are homogeneous with respect to specific properties, such as age, mass, and evolutionary phase.

The study of stellar X-ray coronae, other than the Sun, started a dozen years ago with the launch of the *Einstein* Observatory (Vaiana et al. 1981). From the beginning, a richness of data not anticipated in the original plans for the mission emerged, involving the majority of stellar types and ages. Evidence for evolutionary effects on the stellar X-ray emission was found in the very early observations of the Orion (Ku and Chanan 1979), Hyades (Stern et al. 1981), and Pleiades (Micela et al. 1985) stars. Our effort has been a quantitative description of this behavior. Since then, the major developments of stellar coronal physics have been traced from the data of both *Einstein* and *EXOSAT* observatories, as reviewed, for example, by Vaiana(1983), Rosner, Golub & Vaiana (1985), Vaiana and Sciortino (1987), Pallavicini (1989), Linsky (1990), Vaiana(1990), and references therein.

The new ROSAT observations will undoubtedly complete the present scenario: the complete coverage of the sky will remove some (although not all) of the present observational biases, and the qualitative improvement in spectral response will substantially contribute to a better classification of the nature of the X-ray emission (for some of the new ROSAT all-sky survey results cf. Schmitt 1991, and Schmitt in this issue). Presumably, only the substantial increment in sensitivity attainable with AXAF and XMM will allow other major surprises (see discussion in §4).

Presently the research on stellar coronae has two major subjects: (a) the study of the origin of X-ray emission, and of the variety of its manifestations; (b) the implications that such a variety has on the integrated emission of our Galaxy and of external galaxies, on the diffuse background emission, and on the expected number of stellar coronal sources that will be detected with future more sensitive instruments.

2 Current Knowledge on the Evolution of Stellar Coronal Emission

Most of our present knowledge on stellar X-ray emission is based on the many studies conducted by analyzing representative samples selected out of optical catalogues, hence retaining some of the biases of such samples. For instance, the space volume in which we can study sources depends on the typical distance over which we find them, therefore on their space density. Figure 1 shows the scatter plot of $\log L_x$ vs. distance, for stars of various studied samples (smaller dots indicate upper limits, while distinct symbols refer to different stellar samples). The fact that the brightest sources are the most distant ones reflects this dependence. Already in this representation, however, the Orion, Pleiades and Hyades star samples (identified in Fig. 1 by points aligned at 500 pc, 120 pc, and 45 pc, respectively) tend to be separated in X-rays because of the age-dependence of the stellar X-ray luminosity.

As another instance of parent catalog induced bias figure 2 shows a scatter plot of f_x/f_v vs. m_v for stellar X-ray sources identified with stars in two magnitude-limited catalogs, the BSC ($m_v < 7.1$) and the SAO ($m_v < 10$) catalog, and in the volume-limited Gliese (1969) and Woolley et al. (1970) catalogs, ($distance$ < 25 pc). Note that the stars showing the highest f_x/f_v values are those of the latter catalogs; since they have

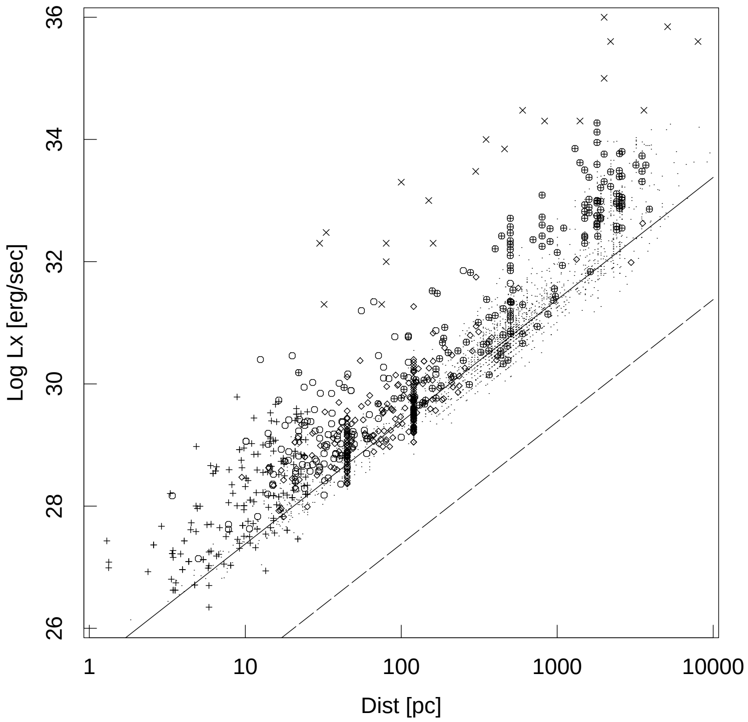

Figure 1: L_x vs. distance for various stellar samples. Detected sources are indicated according to different symbols as follows: Main sequence G, K, M stars (plus), main sequence A-F stars and yellow giants (circles), Orion, Pleiades, Hyades and EMSS stars (diamonds), OB stars (bullets), HEAO-1 compact sources (crosses). Small dots indicate upper limits to the X-ray luminosity. The lines represent limiting sensitivities of 2 10^{-13}erg cm^{-2} s^{-1} (solid), typical of Einstein observations, and of 2 10^{-15}erg cm^{-2} s^{-1} (dashed), expected for the majority of AXAF observations.

on the average small masses and low intrinsic optical luminosities they are absent in the magnitude-limited catalogs.

2.1 Stellar Age as an Ordering Parameter of X-ray luminosity

Quantitative analysis of X-ray emission of stars is obtained by computing X-ray luminosity functions for stellar samples that are statistically representative of stellar population in the solar neighborhood. In Figure 3 we show the maximum-likelihood integral X-ray luminosity functions for dF, dG, and dM field stars (adapted from Schmitt et al. 1985, Maggio et al. 1987, Barbera et al. 1991a,b). The spread in L_x is about two orders of magnitude for the dF dwarfs, and more than three orders of magnitude for the dG and dM stars. We will see (cf. §4) that the tails of the luminosity functions, generally due to the younger component of the samples, are crucial in determining: i) the expected number of coronal sources in a flux limited survey, and ii) the stellar coronal source contribution to the integrated diffuse emission of our Galaxy.

Figure 4 shows the luminosity functions for dK and dM stars, grouped by age (Barbera et al. 1991a,b) according to the kinematical criterion of Eggen (1969), for the Hyades (Micela et al. 1988), the Pleiades (Micela et al. 1990), and for a sample of coeval pre-

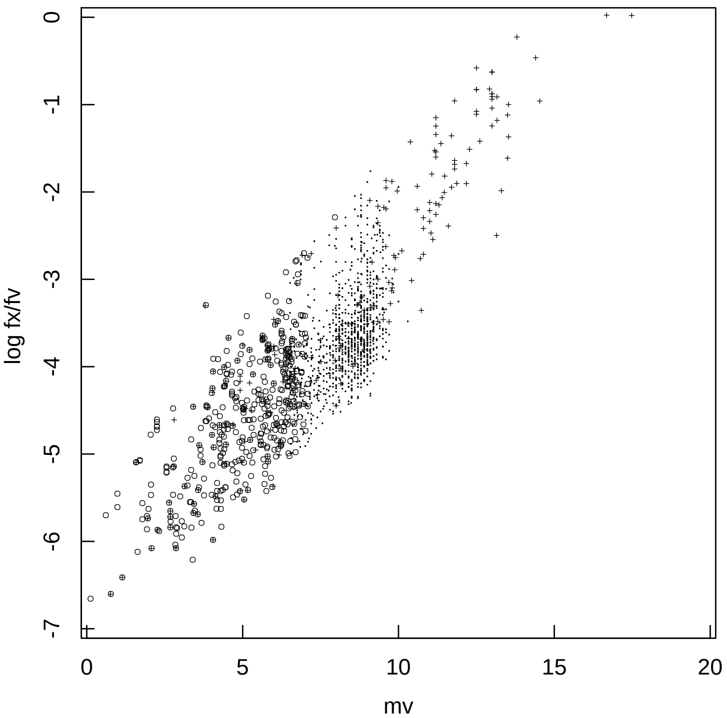

Figure 2: X-ray to visual flux ratio as a function of apparent visual magnitude for identified stellar X-ray sources observed with the *Einstein* satellite. Circles are used for BSC stars, points for stars in the SAO catalog, and plus symbols for Woolley stars. The latter show the highest f_x/f_v values because of the low intrinsic optical luminosity and high X-ray emission level. The lower boundary is determined by the limiting sensitivity of the observations.

main sequence (PMS) stars in the Taurus-Auriga region (Damiani et al. 1990,1991). The spread in L_x is now narrower in each category: in fact, age grouping allows a more clear separation of stars in different L_x ranges. However, the old-disk and young-disk star samples maintain a relatively large spread, likely due to the statistical nature of the criterion used for their separation.

Figure 5 shows the decrease of median $\log L_x$ with stellar age for K and M stars in young associations, in open clusters, and in our neighborhood, starting from the PMS phase – based on the luminosity functions computed by Damiani et al. (1990,1991) for stars in the Taurus-Auriga complex – down to the population of field stars coeval to the Sun. The decrease seems to become steeper for ages greater than $\sim 7 \times 10^8$ yr (the Hyades age), and further indications exist that the rate of decrease of the X-ray emission level may also depend on stellar mass (Micela et al. 1990; Barbera et al. 1991).

2.2 The X-ray Luminosity in the Post Main-Sequence Phase

Recently, we have also improved our knowledge of the post main-sequence variation of the X-ray emission level (Maggio et al. 1990). *Einstein* has observed most of the yellow giants (12 out of 38 with B-V<1) and a sizable fraction of the red giants (9 out of 54) within 25 pc of the sun. The nearest stars were observed with the highest sensitivity ($< 10^{-13}$ erg cm^{-2} s^{-1}). The yellow giants as a whole show evidence of X-ray emission,

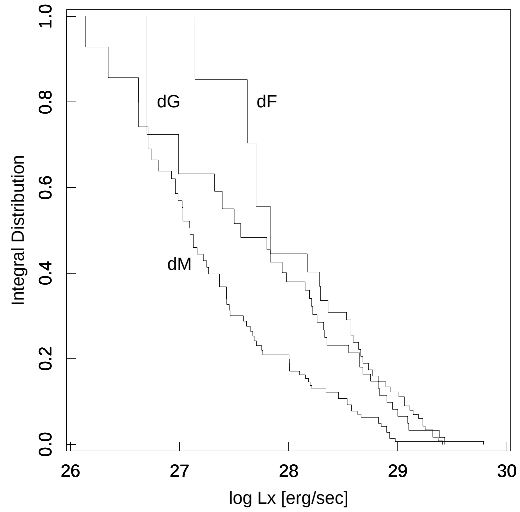

Figure 3: Maximum-likelihood integral X-ray luminosity functions for main-sequence field stars of different spectral types (dF from Schmitt et al. 1985; dG from Maggio et al. 1987; dM from Barbera et al. 1991a,b). Note the increasing range of L_x going from the dF to the dM stars.

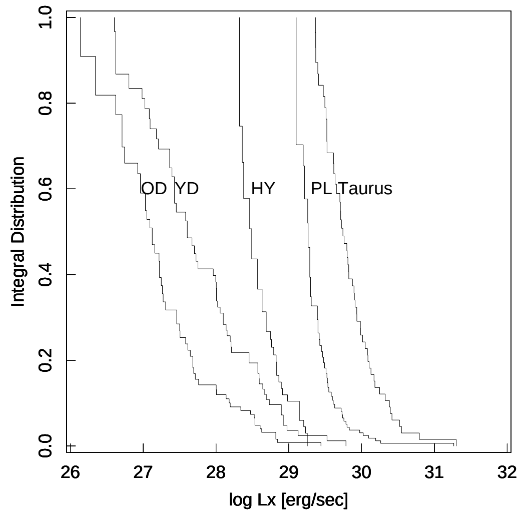

Figure 4: Maximum-likelihood integral X-ray luminosity functions for several coeval samples of main-sequence K and M stars of decreasing stellar age: old disk [OD] and young disk [YD] field stars (data from Barbera et al. 1991a,b), Hyades [HY] (Micela et al. 1988), Pleiades [PL] (Micela et al. 1990), and Taurus-Auriga PMS [Taurus] (Damiani et al. 1990,1991) cluster stars. Notice that the spread of X-ray luminosity reduces significantly when considering stellar samples homogeneous by age.

while the red giants do not (cf. figure 6). In fact, the observed F and G giants have $Mean(\log L_x) = 28.7$ erg s^{-1}, while the K giants have $Median(\log L_x) < 27.6$ erg s^{-1} (in the latter case the luminosity function does not reach the median). The drop at B-V $\sim$ 1 (K0) has been established on a firm statistical ground, and seems to be associated with the ascending phase of the red giant branch.

Such results refer to stars in a wide range of masses (1-5 $M_\odot$). We are now in the

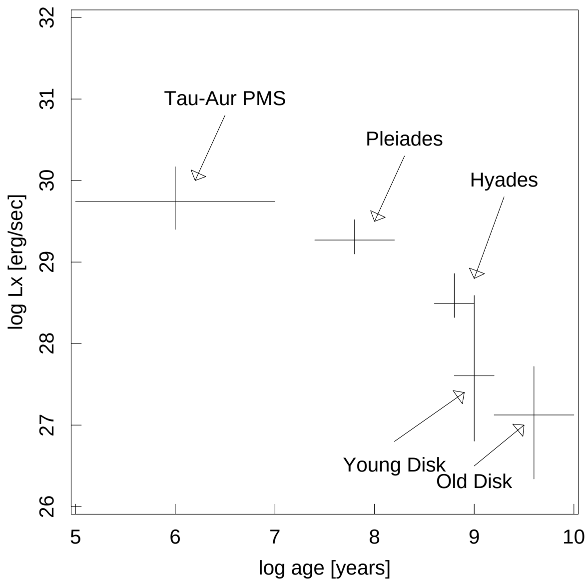

Figure 5: Median X-ray luminosities for K and M stars as a function of stellar age. The median $\log L_x$ values have been computed from X-ray luminosity functions for members of the Taurus-Auriga association, the Pleiades and Hyades open clusters, and for field stars; vertical bars range from 16% to 84% of the distributions. The X-ray emission level clearly decreases with increasing stellar age.

position to begin the exploration of the X-ray emission level for stars in selected narrower mass ranges. In Figure 7 we show the scatter plots of L_x vs. B-V for giants with mass between 1.2 and 1.7 $M_{\odot}$, and between 1.7 and 3.2 $M_{\odot}$. Stellar masses have been estimated from the position in the HR diagram, with respect to evolutionary tracks (Maeder & Meynet 1989) which take into account core overshooting and parameterized mass loss. These two mass ranges were selected because we know the mean L_x – also indicated in the figure – for the main-sequence progenitors. There is a suggestion of an initial increase of L_x followed by a drop at B-V $\sim$ 1, however some active chromosphere stars (mostly RS CVn-like systems) show high X-ray emission level despite their red color. ROSAT observations should be able to improve upon this issue.

The change in the X-ray emission level seems also to be accompanied by a hardening of the X-ray spectrum. In fact, the results of an X-ray spectral survey based on *Einstein* IPC data (Schmitt et al. 1990) indicate that most X-ray luminous giants have coronae with components at T $\sim 10^7$ K, while the main-sequence stars show evidence of coronae with lower temperature components (T $\sim 5 \times 10^6$ K).

The reason for such an evolutionary change could be linked to: a) Changes in the internal structure, in particular deepening (or development) of the convection zone; this may affect the efficiency of a magnetic dynamo mechanism, or trigger the onset of such a mechanism for stars with intermediate-mass main sequence A-type progenitors; b) Expansion of the star envelope and corresponding decrease of the surface gravity; this effect would produce an increase of the coronal pressure scale height, which in turn would influence the thermodynamic and radiative state of the plasma in the outer atmosphere.

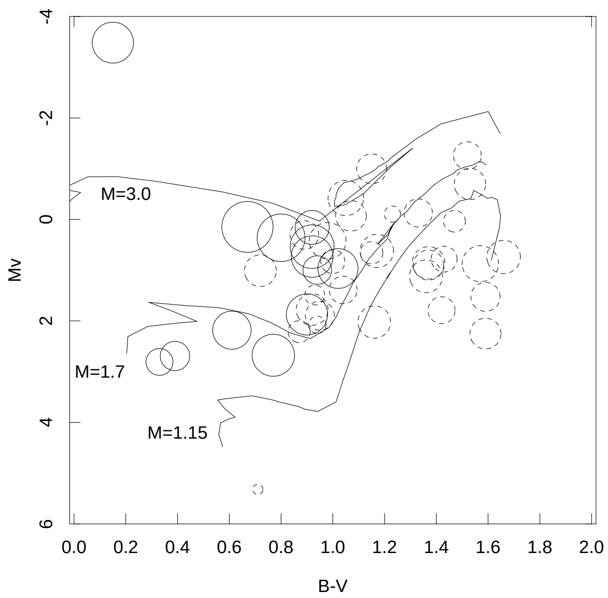

Figure 6: H-R diagram with X-ray detections (solid line circles) and upper limits (dotted line circles) plotted as bubbles whose size is proportional to log L_x. Only non-binary evolved stars within 100 pc are represented. Evolutionary tracks for stars of indicated masses (in units of solar mass) are also shown. Note the 2-3 $M_\odot$ G giants near B-V $\sim$ 0.8, detected at the exit of the Hertzsprung gap.

3 L_x as a tracer of stellar age

Since early observations (Ku and Chanan 1979; Gahm 1980; Feigelson and De Campli 1981; Feigelson and Kriss 1981; Walter and Kuhi 1981, 1984; Montmerle et al. 1983) it has appeared clear that intense X-ray emission is a tracer of young stellar populations. This criterion has allowed the discovery of a new class of young stars, the so called Naked T-Tauri Stars (NTTS; Walter et al. 1988), known also as Weak-line T-Tauri Stars (WTTS; Strom et al. 1989), that have been peeked up due to their intense X-ray emission (Feigelson et al. 1987), and then identified as a class of PMS stars (Walter 1986; Walter et al. 1988).

The adoption of the X-ray luminosity level as a stellar age indicator would result in several advantages:

- easy age classification (at least in a statistical sense) of optically faint stars, if compared with the more traditional spectroscopic or narrow band photometry techniques based on metallicity;

- age determination with a single shot X-ray observation, to be compared with the time and astrometric accuracy necessary using kinematic criteria.

The basis of L_x as an age indicator is strongly supported for disk population main sequence stars by the relationship between the X-ray luminosity level and the kinematic properties of the nearby dK and dM stars. Barbera et al. (1991a, this issue) show in their figure 3 the scatter plot of the U and V space velocity components for their representative sample of X-ray surveyed stars. The ellipse and the polygon divide the U - V space according to the Eggen (1969) criterion. Halo stars populate the velocity region outside

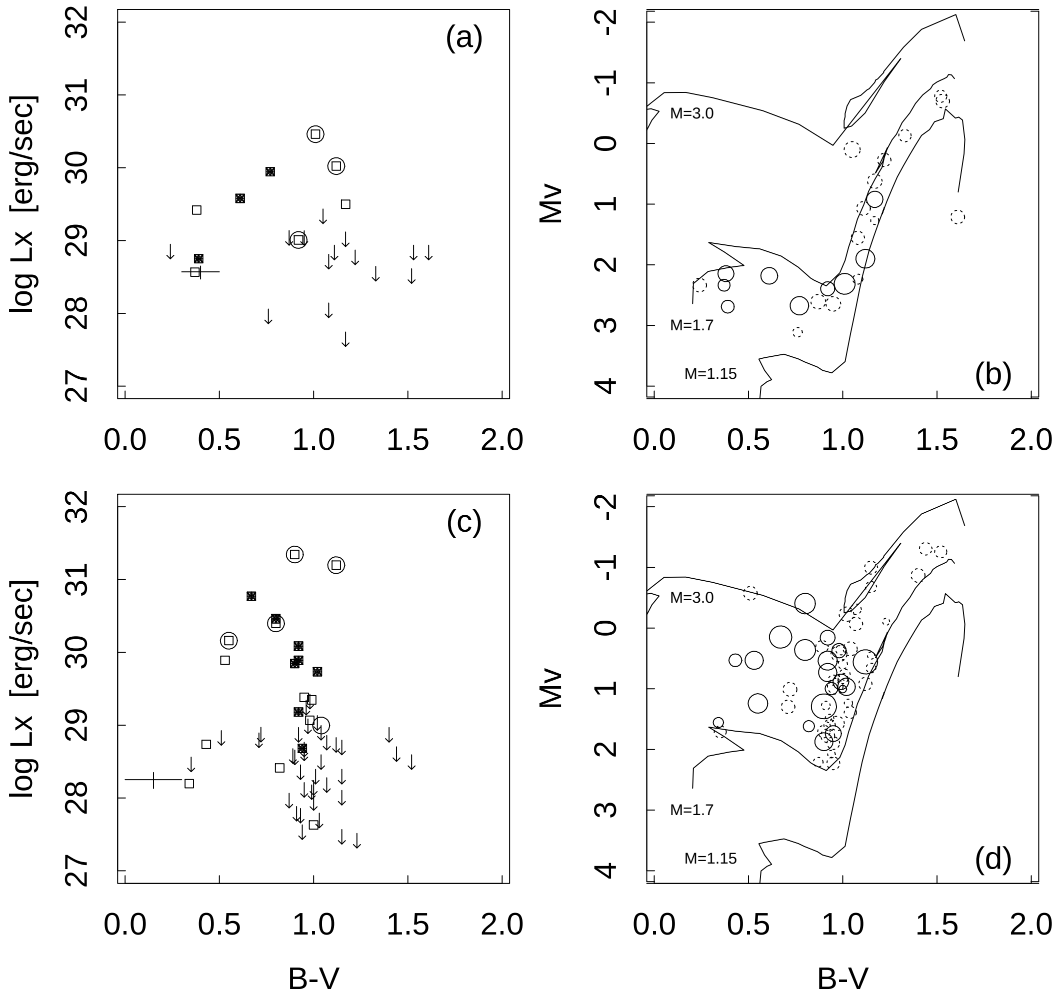

Figure 7: Variation of the X-ray emission level on evolutionary time scales, for stars in two mass ranges. (a) X-ray luminosity vs. B-V color for stars with masses $1.2 < M/M_\odot \leq 1.7$; squares indicate X-ray detections, while arrows indicate upper limits; full squares have been used for presumed single stars, and circles identify RS CVn - like systems; the mean X- ray luminosity for main-sequence stars of similar mass is indicated by a segment. (b) Color-magnitude H-R diagram for the stars in panel (a), where X-ray detections (solid-line circles) and upper limits (dotted-line circles) are plotted as bubbles whose sizes are proportional to log L_x. (c), and (d) are analogous to (a) and (b), respectively, but for stars in the mass range $1.7 < M/M_\odot \leq 3.2$. These plots suggests an initial increase of the X-ray emission level, followed by a drop near the base of the red giant branch (B-V $\sim$ 1).

the ellipse, the young disk stars the region inside the polygon, and the old disk stars the region between the ellipse and the polygon. *The stars with $L_x \geq 10^{27.6}$ erg s^{-1} tend to have small velocities, i.e they have, as a class, kinematical properties of the young-disk population.*

Recently the relationship between L_x and classical age indicators (kinematic and

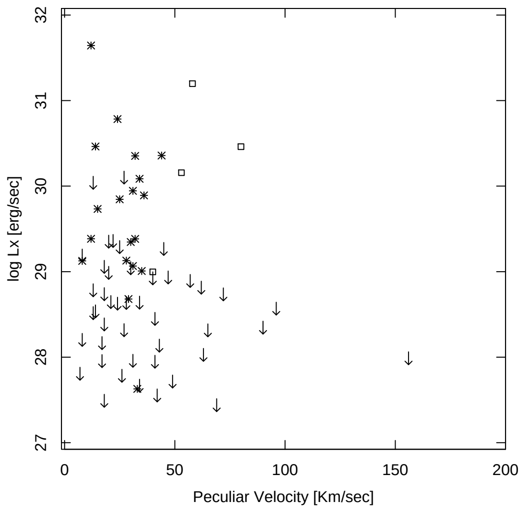

Figure 8: Scatter plot of X-ray luminosities versus peculiar velocities for G and K giant stars. Arrows indicates upper limits in L_x; square symbols indicate stars classified as RS CVn - like systems. The high X-ray luminosity stars tend to have lower peculiar velocities than the low X-ray luminosity stars.

metallicity) have been explored for a sample of yellow disk giants (Micela, Maggio & Vaiana 1991). Figure 8 shows a scatter plot of $\log L_x$ vs. peculiar velocity, i.e. the star velocity with respect to the LSR, for a sample of yellow disk giants taken from the classical work of Roman (1952) and observed with the *Einstein* Observatory (Maggio et al. 1990). It is evident that the giants with high L_x tend to have smaller mean velocities and a lower dispersion with respect to those with low L_x. Notice that the four RS CVn - like systems in this sample (indicated with square symbols) show an anomalous behavior.

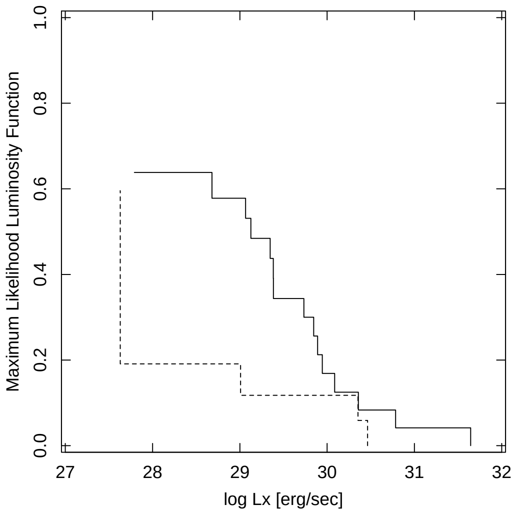

Figure 9: Maximum-likelihood integral X-ray luminosity functions for strong-lined (solid line), and weak-lined (dotted line) G-K giants. The two distributions are statistically distinguishable at the 98% confidence level.

A similar result is obtained computing the X-ray luminosity functions of strong-lined and weak-lined giants. The two luminosity functions, shown in figure 9, are significantly different and the $Mean(\log L_x)$ values differ by one order of magnitude. *These two results taken together suggest that the X-ray luminosity level is an age indicator for yellow giants as good as the kinematic and metallicity criteria.*

4 Coronal Emission and Stellar Population: the XCOUNT Galaxy Model

XCOUNT is a numerical model built up by our group in Palermo, and collaborators at ESA, for predicting and studying the stellar X-ray emission components of our Galaxy (Favata et al. 1992). From the optical point of view, it is based on the Bahcall & Soneira Galaxy model (Bahcall & Soneira 1980; Bahcall 1986) which assumes the Galaxy being formed by a disk and a spheroidal component. The density of stars in the disk is schematically assumed to be an ellipsoid with maximum density and scale height depending on spectral type and radial scale length dependent on the galaxy type.

In the present model implementation, we have decided to consider only giant and main sequence stars of disk population, since we have little knowledge of the X-ray luminosity function of halo stars. Such a choice is supported by the sparse (up to date) X-ray observations that indicate old population stars as low level X-ray emitters: in particular, halo stars in our neighborhood (such as the Barnard star) are among the lowest X-ray emitters known to date. However, the sensitivity of the *Einstein* observations did not allow to sample *even* the tail of the distribution of such low-density halo stars. Hence, the above indications need to be confirmed by larger size samples like those that will be available with the ROSAT all-sky survey and, probably better, by future more sensitive observations (such as those foreseeable with AXAF and XMM).

The X-ray information is largely summarized in the maximum likelihood X-ray luminosity functions determined over the past decade largely by our group (cf. Schmitt et al. 1985; Micela et al. 1985; Maggio et al. 1987; Micela et al. 1988; Feigelson & Kriss 1989; Maggio et al. 1990; Micela et al. 1990; Sciortino et al. 1990; Damiani et al. 1990, 1991; Barbera et al. 1991a,b; Grillo et al. 1991a,b), as a function of spectral type and age.

The remaining ingredient we have incorporated in our model is an analytic description of the galactic hydrogen density (Lockman 1984) parameterizing the X-ray absorption by interstellar gas with an assumed abundance of heavy elements relative to hydrogen.

The XCOUNT X-ray Galaxy model is characterized by its portability, flexibility and extensibility. It is written in C modules. The instrumental characteristics, the HR diagram, the luminosity functions, are all external tables to the program and can be easily changed. Presently, tables for the *Einstein* IPC and the ROSAT PSPC are available to perform computations.

4.1 Analysis of the Stellar content of EMSS

The color and the magnitude distributions predicted by XCOUNT model (Favata et al., 1991a,b) have been compared to the observed ones in the *Einstein* Extended Medium Sensitivity Survey (EMSS; Gioia et al. 1990; Fleming 1988; Stocke et al. 1991).

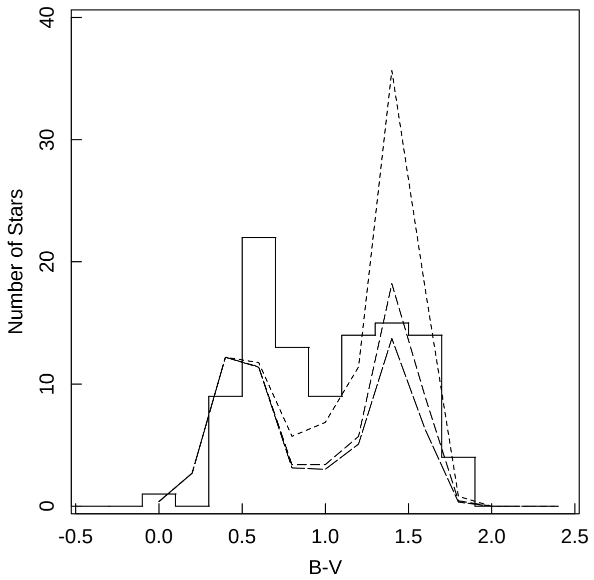

Figure 10: Observed and predicted B-V color distributions for X-ray sources in the EMSS. Three different predictions are shown, obtained with the Palermo-ESA XCOUNT Galaxy Model, based on different assumptions for the content of young- and old-disk stellar populations: a single stellar disk population (short-dashed line); an old-disk component plus a young-disk component with scale height and density being 0.5 and 0.1, respectively, of the old one (long dashed); an old-disk and a young-disk component mix-up following a constant birth rate (medium-dashed). Evolutionary effects must be taken into account to reproduce the observed star counts for the M stars. Observations show also an excess of yellow stars, whose origin is still not completely understood.

The predicted distributions, shown in figure 10, are based on three different hypotheses for the spatial distribution of the stars, namely:

1. The luminosity functions do not depend on stellar age (short-dashed line). In this case the stellar density is computed assuming a single scale height for each spectral type, i.e. we assume the same stellar disk population of the original Bahcall & Soneira model.

2. The luminosity functions do depend on stellar age. In this case we assume a young disk and old disk populations, with scale height and density for the young component being 0.5 and 0.1 of old ones, respectively (long-dashed line).

3. Same as above, but with density of the young component in the Galaxy plane being 0.2 of the old one (medium-dashed line). This choice corresponds approximately to assuming a constant stellar birth rate in the solar neighborhood.

The comparison of these predictions with actual observation (cf. figure 10) shows that:

- Evolutionary effects of the X-ray emission must be included to account for the observed stellar counts of M stars in the EMSS.

- Observations show an excess of yellow stars in the EMSS with respect to prediction, confirming previous conclusion based on a early version of the model and a smaller data set (Favata et al. 1988).

With reference to this last point we notice that the observed excess cannot be explained by normal giants, and that the subsample, we have adopted for comparison, does not contain all known RS CVn's, W UMa, and PMS stars. Only if a large number of such objects have not been recognized yet, they can account for the observed excess. If this is the case, their space density requires to be substantially larger than the currently accepted value. The ongoing program of optical follow-up studies of serendipitous stars seen with the EXOSAT-CMA detector suggests that many of them are PMS or RS CVn-like systems (Pallavicini, 1991; private comunication). A similar indication results from the ongoing program of optical follow-up studies of southern EMSS stars, we have recently undertaken (Favata et al. 1991c). Another viable possibility is that the available X-ray luminosity functions of yellow stars severely undersample young active main sequence stars.

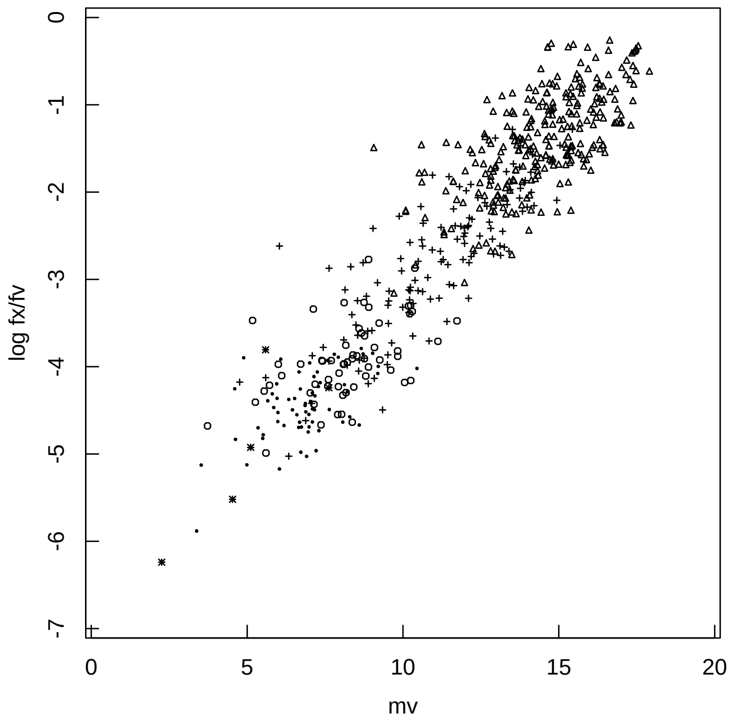

Figure 11: Model predictions of the $\log f_x/f_v$ vs. m_v distribution of the 523 X-ray sources detectable in all the *Einstein* IPC fields, assuming a mixing of young-disk and old-disk populations corresponding to a constant stellar birth rate in our neighborhood. Different symbols indicate main sequence stars of spectral types A-F (dot), G (circle), K (plus), M (triangle), and disk giants of spectral type G and K (asterisk).

4.2 Prediction of Stellar Coronal Source Number Counts

The Galaxy model allows also to generate simulations of the expected scatter plot of $\log f_x/f_v$ vs. m_v for a given set of observations. We have used the model to generate a simulation of the bidimensional log f_x/f_v - m_v distribution of the 523 X-ray detectable sources in all the $\sim$ 4000 *Einstein* IPC pointings taking into account the sensitivity of each individual field and the subdivision in three distinct age ranges.

Figure 11 shows the result of such a simulation distinguishing different spectral types: A, F, G, K, and M (including the separate contributions from M stars with absolute visual luminosity $<$ 13.5, M_b, and $>$ 13.5, M_r). Notice that the range of m_v and f_x/f_v is well defined for each spectral class. The lower envelope of the predicted scatter plot is determined by the values of the limiting sensitivity of observations. Most of the spread in the direction orthogonal to lines of constant X-ray flux, is accounted for by the width of the X-ray luminosity functions (3 orders of magnitude) plus the spread in the optical luminosity function (less than 1 order of magnitude for G stars, $\sim$ 1 order of magnitude for K and M_b stars, and $\sim$ 2 orders of magnitude for M_r stars). The spread in X-ray limiting sensitivities smoothes out the expected clustering of sources in the low flux region.

Figure 12 shows a similar simulation putting in evidence with different symbols young and old disk K and M star sources. Young stars are on the average at greater f_x/f_v values than old stars.

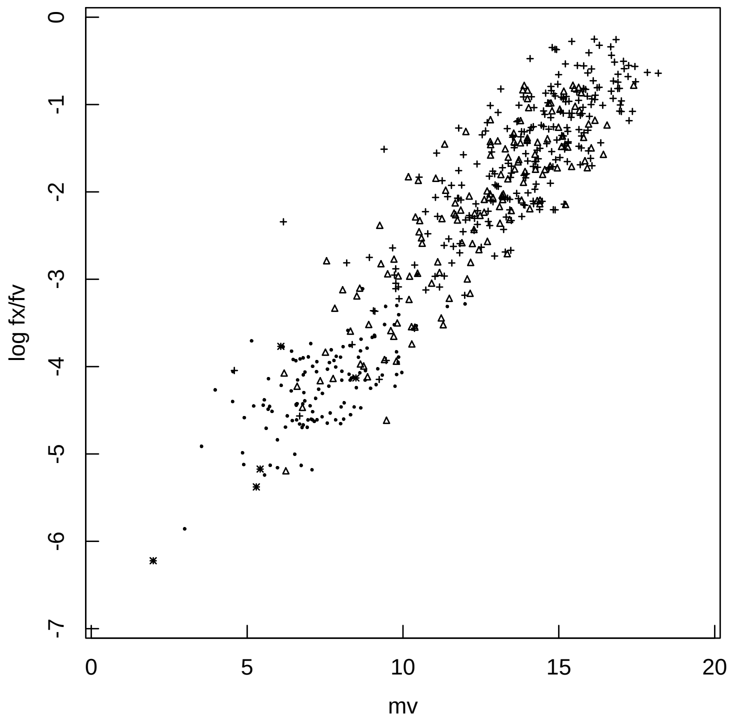

Figure 12: Same as previous figure, but with spectral types and stellar ages coded as follows: young-disk main sequence K and M stars (plus), old-disk main sequence K and M stars (triangle), main-sequence A, F, and G (dot) stars, and disk giants of spectral type G and K (asterisk). Note that the young stars tend to be at larger f_x/f_v values than the old stars.

As a result of stellar density scale heights, and shape of X-ray luminosity functions, if we had a very large X-ray sensitivity, we would expect a *clustering of stars* in the f_x/f_v vs. m_v plane for each pointing direction. Based on our X-ray Galaxy model, the expected positions of the centroids of the distributions in the f_x/f_v, m_v plane, at $b = 20°$ and $l =$

90°, are listed in the following table for various spectral type and, eventually, for old-disk (subscript o) and young-disk (subscript y) population stars.

PREDICTED m_v - $\log f_x/f_v$ CENTROID FOR DISTINCT SPECTRAL TYPES at $b = 20°$ and $l = 90°$

Spectral Type	A	F	G	K_y	K_o	M_{by}	M_{bo}	M_{ry}	M_{ro}
m_v	12	15	16	18	19	21	22	24	26
$\log f_x/f_v$	-6.50	-5.50	-4.62	-4.00	-4.62	-2.75	-4.00	-1.50	-2.75

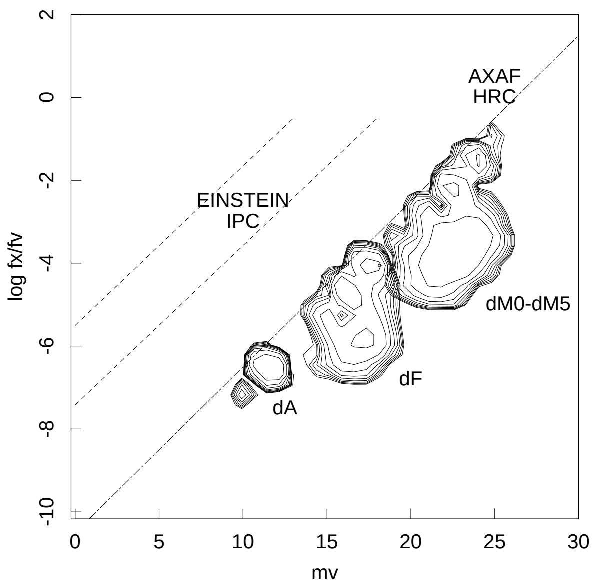

Figure 13: Model-predicted density contour maps in the $\log f_x/f_v$ - m_v plane, for stars of various spectral types observable at $b = 20°$, and $l = 90°$. For comparison, are shown the range of limiting sensitivities achieved by the *Einstein* IPC observations, and the foreseeable limiting sensitivities for the AXAF HRC. It is noteworthy that even AXAF will not be able to reach the centroid of the distribution of M stars.

Figure 13 shows the density contour map (number of star per unit m_v, and unit f_x/f_v) for the dA, dG, dM_b stars at $b = 20°$ and $l = 90°$. The density of each group has been normalized to the individual maximum values, and the contours cover the range between 1 and 1/10 of this value.

The centroid positions have also a dependence on latitude: at the poles they will move towards smaller m_v values (apparently more luminous stars), and at the plane they will move towards larger m_v values (less luminous stars). The limiting flux required to get the centroids is very low: for instance, at $b = 20°$, we predict $f_x \sim 10^{-(17 \div 18)}$ erg cm^{-2} s^{-1}, that should become $f_x \sim 10^{-(16 \div 17)}$ erg cm^{-2} s^{-1} at the pole. The number of stars per square degree is very high and obviously there will be source confusion at presently foreseeable sensitivity and resolution. As shown in figure 13, *AXAF will detect only the* *tail of the stellar distribution of M stars, hence even AXAF will not be able to image the stellar soft X-ray background in a resolved manner.*

4.3 The stellar contribution to the diffuse soft X-ray background and the origin of the Galactic Ridge.

Since the seminal paper of Rosner et al. (1981), based on actual detections of soft X-ray emission from ordinary solar-like stars, several authors have evaluated and discussed the contribution of stellar coronal source to the diffuse soft X-ray background (Caillault et al. 1986, Caillault 1990, Schmitt & Snowden 1990). Recently, Kashyap et al. (1992) have done a detailed calculation taking into account the space distribution of stars in the Galaxy, the detailed distribution of hydrogen particle along the line of sight, a two temperature and a continuous emission measure model for stellar coronal sources, and the full set of X-ray luminosity functions available at the end of 1990.

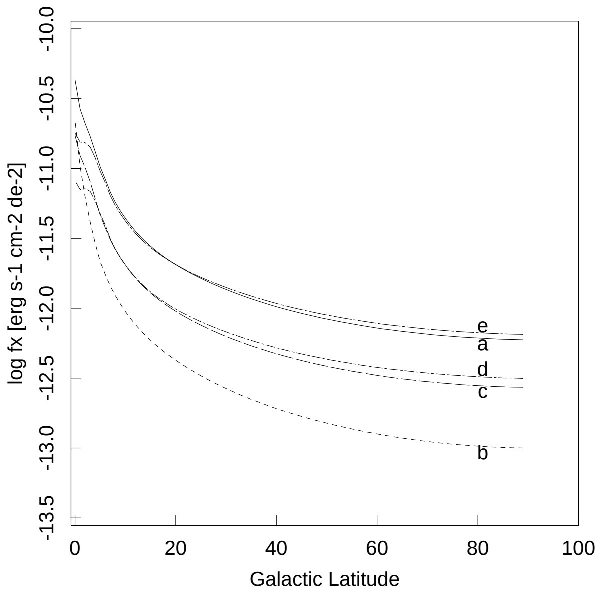

Figure 14: Predicted contribution of unresolved coronal sources as a function of galactic latitude for a limited X-ray flux of 10^{-13}erg cm^{-2} s^{-1} (line *a*). The contributions from the three different stellar populations considered are also shown: "Pleiades-age" (line *b*), "Hyades-age" (line *c*), and "Old-Disk Population" (line *d*) stars. For comparison, we shows the predicted contribution assuming a single stellar population modeling (line *e*).

More recently, we have adopted XCOUNT to re-evaluate the prediction of the stellar contribution to the diffuse soft X-ray background (Micela 1991, Sciortino 1991, Micela et al. 1991a). The prediction shown in figure 14 has been evaluated for $f_x \sim 10^{-13}$ erg cm^{-2} s^{-1} – a typical *Einstein* Observatory limiting sensitivity – in the energy band 0.16 - 3.5 keV, under the following hypotheses, that try to make the best usage of now available X-ray information:

- The nearby dA-dF field stars are representative of the dA-dF stars in the entire Galaxy.

- The dG, dK, dM stars have been divided into 3 age ranges whose characteristics are listed below:

Age (yr)	Scale Height (pc)	Prototype X-ray Lum. Fun.	Coronal Temp. (keV)
$10^7 - 10^8$	140	Pleiades	1.1
$10^8 - 10^9$	240	Hyades/Young Disk	0.5
$10^9 - 10^{10}$	400	Old Disk	0.3

- Stellar density in the Galactic plane has been derived assuming a constant birth rate.
- Coronal temperature has been been changed according to stellar age, as indicated above.

This model seems to explain the Galactic Ridge emission in terms of unresolved coronal emission from young stars, and predicts that the stellar contribution toward galactic poles is only few percent of the observed diffuse soft X-ray background in the (0.16 - 3.5 keV) energy band. However, we notice that the inclusion of halo population stars could result in a different make-up at significantly lower limiting fluxes, with some change in the predicted stellar contribution especially toward poles. In figure 15 (line e) we show a similar calculation but without taking into account evolutive effects, and with coronal temperature fixed to kT = 0.3 keV. In this case the model still predicts an increase of the emission in the galactic plane, but the prediction accounts only for $\sim 25\%$ of the observed excess X-ray emission in the Ridge.

In figure 15 we show the comparison of the Galactic Ridge model prediction and the actual IPC background measurements as a function of galactic longitude for the region of sky confined to the $|b| < 5^\circ$ strip. The bullets are experimental data taken from the *Einstein* IPC survey of soft X-ray background (Micela et al. 1991b), and the lower and upper lines are the predicted profiles computed for $b = 0^\circ$ and $b = 5^\circ$, respectively, summed up to the average level of instrumental contamination (dashed line).

Future more sensitive, high resolution observations covering the energy range up to about 10 keV, such as those that will be available with the AXAF and XMM missions, will allow to better probe the origin of the Galactic Ridge. In particular, the origin of the iron 6.7 keV emission line discovered in star formation regions with the few degrees spatial resolution instrument of Ginga (Koyama 1988a,b) is an open and intriguing research problem.

Acknowledgments: We thank M. Barbera and F. Favata for having provided material in advance of publication, and our colleagues A. Collura, F. Reale, and S. Serio for their critical reading of this paper. We acknowledge support from Ministero della Università e della Ricerca Scientifica e Tecnologica, and from Agenzia Spaziale Italiana.

References

Bahcall, J. N. 1986, Ann. Rev. Astron. Astrophys., 24, 577.

Bahcall, J. N. and Soneira, R. M. 1980, Ap. J. Suppl., 44, 73.

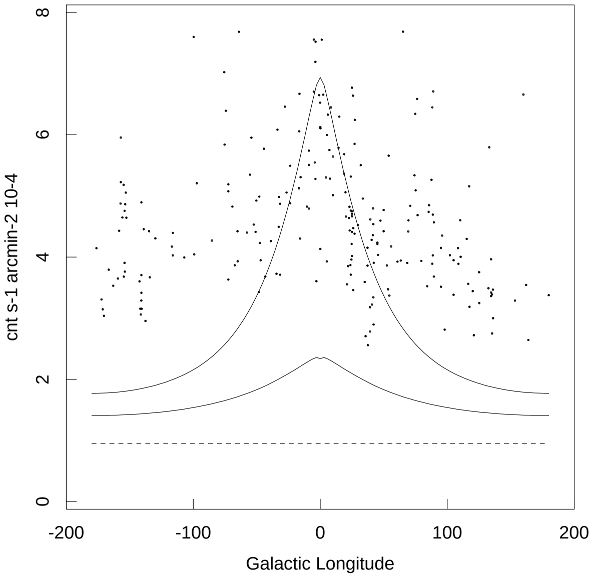

Figure 15: Comparison of a model prediction of the soft X-ray background galactic ridge with *Einstein* Observatory IPC measurements, in the region of sky with $|b| < 5°$. The dashed line is the average level of non-astrophysical contamination. The lower and upper solid lines are the predicted profiles computed for $b = 0°$ and $b = 5°$, respectively.

Barbera, M., Micela, G., Sciortino, S., Vaiana, G. S., Harnden, F. R., Jr., and R. Rosner 1991, Mem. Soc. Astr. It., this issue.

Barbera, M., Micela, G., Sciortino, S., Vaiana, G. S. Harnden, F. R., Jr., and R. Rosner 1991, Ap. J., in preparation.

Damiani, F., Micela, G., and Vaiana, G. S. 1990, In Catalano, S., and Stauffer, J. R., editors, *Angular Momentum Evolution of Young Stars*, page 89, Kluwer Academic Publishers

Damiani, F., et al. 1991, in preparation.

Eggen, O.J. 1969, P.A.S.P., 81, 553.

Favata, F., Rosner, R., Sciortino, S., and Vaiana, G. S. 1988, Ap. J., 324, 1010.

Favata, F., Micela, G., Sciortino, S., and Vaiana, G. S. 1991a, In Tanaka, Y. and Koyama, K., editors, *Frontiers of X-ray Astronomy*, page in press, Tokio. Universal Academy Press, Inc.

Favata, F., Micela, G., Sciortino, S., and Vaiana, G. S. 1991b, in preparation.

Favata, F., Barbera, M., Micela, G., Sciortino, S. 1991c, in preparation.

Favata, F., Micela, G., Sciortino, S., and Vaiana, G. S. 1992, A&A, in press.

Feigelson, E. and Kriss, G. A. 1981, Ap. J., 248, L35.

Feigelson, E. and De Campli, W. M. 1981, Ap. J., 243, L89.

Feigelson, E. D., Jackson, J. M., Mathieu, R. D., Myers, P. C., and Walter, F. M. 1987, A. J., 94, 1251.

Feigelson, E. and Kriss, G. A. 1989, Ap. J., 338, 262.

Fleming, T. H. 1988, PhD Thesis, University of Arizona.

Gahm, G. F. 1980, Ap. J., 242, L163.

Gioia, I. M., Maccacaro, T., Schild, R. E., Wolter, A., Stocke, J., Morris, S., and Henry, J. P. 1990, Ap. J. Suppl., 72, 567.

Gliese, W. 1969, Veroffentlichungen des Astronomishen Rechen-Institus 22, University of Heidelberg.

Grillo, F., Sciortino, S., Micela, G., Vaiana, G. S. and Harnden, F. R., Jr. 1991a, Mem. Soc. Astr. It., this issue

Grillo, F., Sciortino, S., Micela, G., Vaiana, G. S. and Harnden, F. R., Jr. 1991b, Ap. J., in preparation.

Kashyap, V., Rosner, R., Sciortino, S., Micela, G., Vaiana, G. S., Harnden, F. R., Jr. , 1992, Ap. J., in press.

Koyama, K. 1988a, Comments Astrophys., 12, 287.

Koyama, K. 1988b, ISAS Res. Note n. 391.

Ku, W. H. M., and Chanan, G. A. 1979, Ap. J. Lett., 234, L59.

Lockman, F. J. 1984, Ap. J., 283, 90.

Linsky, J. 1990, in Elvis, M., editor, *Imaging X-ray Astronomy*, page 39. Cambridge University Press.

Maeder, A., and Meynet, G. 1988, Astr. Ap. Suppl., 76, 411.

Maggio, A., Sciortino, S., Vaiana, G. S., Majer, P., Golub, L., Bookbinder, J., Harnden, F. R., Jr., and Rosner, R. 1987, Ap. J., 315, 687.

Maggio, A., Vaiana, G. S., Haisch, B. M., Stern, R. A., Bookbinder, J., Harnden, F. R., Jr., and Rosner, R. 1990, Ap. J., 348, 253.

Micela, G., Sciortino, S., Serio, S., Vaiana, G. S., Bookbinder, J., Golub, L., Harnden, F. R., Jr., and Rosner, R. 1985, Ap. J., 292, 172.

Micela, G., Sciortino, S., Vaiana, G. S., Schmitt, J. H. M. M., Stern, R. A., Harnden, F. R., Jr., and Rosner, R. 1988, Ap. J., 325, 798.

Micela, G., Sciortino, S., Vaiana, G. S., Harnden, F. R., Jr., Rosner, R., and Schmitt, J. H. H. M. 1990, Ap. J., 348, 557.

Micela, G. 1991, Ph.D. Thesis, University of Palermo.

Micela, G., Sciortino, S., M. Barbera, F. Favata, and Vaiana, G. S. 1991a, in preparation.

Micela, G., Harnden, F. R., Jr., Rosner, R., Sciortino, S., and Vaiana, G. S. 1991b, Ap. J., 380, 495.

Micela, G., Maggio, A., and Vaiana, G. S. 1991, Ap. J., in press.

Montmerle, T., Koch-Miramond, L., Falgarone, E., and Grindlay, J. 1983, Ap. J., 269, 182.

Pallavicini, R. 1989, Astr. Ap. Rev., 1, 177.

Parker, E. N. 1979, In *Cosmical Magnetic Fields*, Clarendon, Oxford.

Roman, N. 1952, Ap. J., 116, 122.

Rosner, R., Golub, L., and Vaiana, G. S. 1985, Ann. Rev. Astr. Astroph., 23, 413.

Rosner, R., Low, B. C., and Holzer, T. E. 1986, In *Physics of the Sun*, Vol. II, p. 135, Reidel, Dordrecht.

Schmitt, J. H. M. M., Golub, L., Harnden, F. R., Jr., Maxson, C. W., Rosner, R., and Vaiana, G. S. 1985, Ap. J., 290, 307.

Schmitt, J. H. M. M., Collura, A., Sciortino, S., Vaiana, G. S., Harnden, F. R., Jr., and Rosner, R. 1990, Ap. J., 365, 704.

Schmitt, J. H. M. M. 1991, In *Proc. VII Cool Star Workshop*, M. Giampapa editor, in press.

Sciortino, S., Vaiana, G. S., Harnden, F. R., Jr., Ramella, M., Morossi, C., Rosner, R., and Schmitt, J. H. H. M. 1990, Ap. J., 361, 621.

Sciortino, S. 1991, Invited Talk at the Meeting "Statistical Challenges in Modern Astronomy", Penn State University, August 1991

Stern, R. A., Zolcinski, M. C., Antiochos, S. C., and Underwood, J. M. 1981, Ap. J., 249, 647.

Stocke, J. T. et al. 1991, Ap. J. Suppl, 76, 813.

Strom, K. M., Strom, S. E., Edwards, S., Cabrit, S., Skrutskie, M. F. 1989, A. J., 97, 1451.

Vaiana, G. S., Cassinelli, J. P., Fabbiano, G., Giacconi, R., Golub, L., Gorenstein, P., Haisch, B. M., Harnden, F. R., Jr., Johnson, H. M., Linsky, J. L., Maxson, C. W., Mewe, R., Rosner, R., Seward, F., Topka, K., and Zwaan, C. 1981, Ap. J., 245, 163.

Vaiana, G. S. 1983, In Stenflo, O., editor, *Solar and Stellar Magnetic Fields. Origins and Coronal Effects*, page 165, Dordrecht. Reidel.

Vaiana, G. S. and Sciortino, S. 1987, In *Circumstellar Matter, IAU Simp. 122*, page 333. Reidel Publishing Co.

Vaiana, G. S. 1990, in Elvis, M., editor, *Imaging X-ray Astronomy*, page 61. Cambridge University Press.

Walter, F. M., Kuhi, L. V. 1981, Ap. J., 250, 254.

Walter, F. M. 1986, Ap. J., 306, 573.

Walter, F. M., Brown, A., Mathieu, R. D., Myers, P., and Vrba, F. J. 1988, A. J., 96, 297.

Woolley, R., Epps, E. A., Penston, M. J. and Pocock, S. B. 1970, Royal Obs. Ann., 281, 815.